

# The Physics of Design and Operation of High Power Neutral Beam Injection Ducts – Extrapolating JET Experience to ITER Situations

T. T. C. Jones, E. Surrey

UKAEA/Euratom Fusion Association, Culham Science Centre, Abingdon, OX14 3DB, UK

timothy.jones@jet.uk

**Abstract.** Neutral beam injection systems have proven to be the single most effective form of heating for tokamak plasmas. Typical beam pulse lengths are of the order of ten seconds and the major limitation to increased pulse length in multi-megawatt beamlines is the effect of re-ionised neutral particles in the restricted drift space, or “duct”, connecting the beamline to the tokamak vessel. These particles are deflected and frequently focused by the stray magnetic field of the tokamak and can produce significant power density on the walls of the duct. In JET the power density due to re-ionisation can reach ten megawatt per square metre and is the main limitation to beam pulse length. The effect of the re-ionised power is to cause local heating of the duct wall and evolution of gas trapped within the wall material. This raises the pressure in the duct, causing further re-ionisation of the beam and hence increased wall heating. Unchecked, this process can lead to complete re-ionisation of the beam and possible structural failure of the duct wall. A new model is presented that describes an effective source rate of excess gas evolved from the wall in terms of the surface temperature and area subjected to heating. This approach reduces the predicted dependency of duct pressure on beam flux relative to conventional models, parametrised by an ion-induced desorption coefficient, and is validated by comparison with measurements from the 80keV and 130keV JET beamlines over similar power ranges. In conjunction with a particle trajectory re-ionisation code to determine the size and power loading of the affected area, a self-consistent description of the duct pressure balance may be determined for a given heat-transfer characteristic at the wall. This can be directly applied to the design of systems for ITER such as the duct liner and the electrostatic residual ion dump panels. The time response of the duct pressure can be used to establish the mechanism by which gas is released. It is shown that only the percolation of occluded gas within the structure of the wall can account for the timescale over which the pressure is observed to rise and the quantity of gas released. These occlusions occur as a result of localised damage within the wall material and hence it follows that gas evolution will be a function of the ageing process of future systems.

## 1. Introduction

For present day beamline systems with total powers of several megawatts the typical pulse length is of the order ten seconds, and for ITER a high power long pulse system is foreseen (16.7MW per beamline for up to one hour). The high power beams are injected through a restricted drift tube known as the NB Duct (NBD), joining the injector and tokamak vacuum envelopes. The space is necessarily restricted due to the need to keep minimum circumferential distance between adjacent toroidal field coils (to minimise toroidal field ripple), and pairs of vertical poloidal field coils. In the ITER NBD there are additional restrictions in NBD height arising from the blanket module and shielding elements. These space restrictions lead to extremely high power densities:  $\sim 60 \text{ MWm}^{-2}$  in the case of ITER, and over  $300 \text{ MWm}^{-2}$  in the JET system. In the NBD a fraction of the neutral beam is re-ionised by collision with the residual gas molecules, and the resulting charged particles are deflected by the tokamak's stray magnetic field, impinging on the NBD wall. The dominant focusing effect is from the vertical field, and hence the position of the focus depends mainly on plasma current (*FIG.1*). However, the degree of focusing and shape of the deposited power distribution has a very complex dependence on the precise plasma configuration, and can only be predicted accurately by using a 3D Monte Carlo trajectory calculation code. In addition the NBD, as final beam-defining aperture, is subject to power loading from direct interception (or ‘scraping’) in the neutral beam periphery; with the present JET beams the directly intercepted beam fraction is about 3%. The NBD is therefore an especially critical beamline component, due to its restricted geometry and consequent limited conductance for gas evolved through

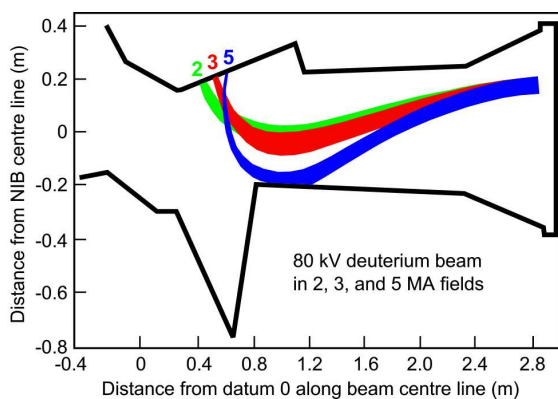


FIG. 1. Schematic map of re-ionised power trajectories in plan representation of JET NBD. Ions born upstream are focused as shown at plasma currents indicated; ions born throughout duct region (not shown) produce a more diffuse distribution. Note X and Y scales not the same.

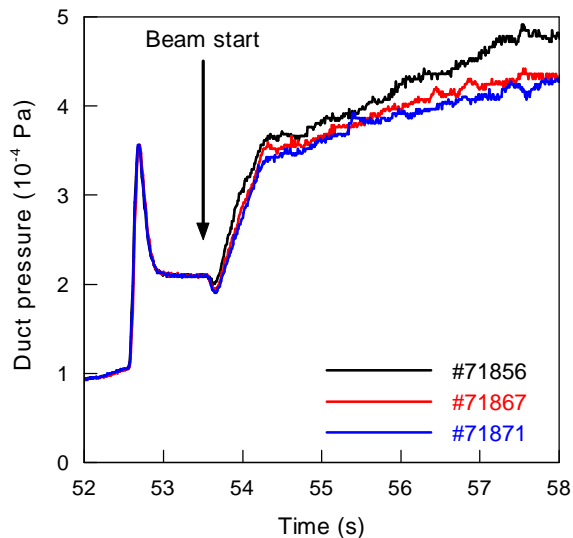


FIG. 2. Duct pressure evolution for well conditioned JET duct (80keV beams) at identical power (9 MW starting at 53.5s; neutraliser gas valves open at 52.5s) and identical torus gas fuelling conditions, showing slow linear rise phase and small shot to shot reduction.

dumping of the lost beam particles and thermal gas desorption from the heated surfaces. This paper uses operational experience on JET, and developments in describing the thermal gas release arising from the physics design of a new actively cooled NBD for JET, for extrapolation to ITER, and analyses the consequences for aspects the ITER beamline design. This applies not only to the NBD but also to components such as the Electrostatic Residual Ion Dump (ERID) proposed for ITER where beam is dumped within narrow channel geometry.

## 2. Physics Design of Actively Cooled Upgraded JET Duct Protection

The presently installed JET duct protection consists of plates of OFHC copper mounted on a stainless steel support structure located within a main horizontal port of the vacuum vessel; the design is described in [1]. The copper plates rely on thermal inertia to absorb the deposited energy with brazed cooling tubes on the rear side to remove the heat between pulses. The thickness varies with position, up to 4.5cm. The plates are extensively instrumented with thermocouples. New actively cooled NB duct protection [2] has been designed to cater for the increased beam power and pulse length following completion of the JET EP2 NB Enhancement [3]. A key design requirement was to ensure that the heat transfer performance of the surface of the duct protection panels is adequate to maintain a large margin against thermal stress related fatigue, or even burnout. This required a reliable prediction of the re-ionised power density which in turn depends on the gas re-emission characteristics in combination with the upgraded beam parameters, especially beam particle flux. Using the extensive amount of operational data from the existing JET duct (Penning gauge and thermocouple measurements) the gas-balance model [1] and its further developments could be benchmarked. The key feature of the model [1] is the assumption of a constant (though adjustable) gas re-emission coefficient,  $\Gamma$ . That is, the gas production rate, and hence steady-state pressure during beam injection, should depend on only total beam flux and re-ionisation cross-section under otherwise similar conditions. Due to the fact that JET's two beamlines

operate at similar power but significantly different voltages (80kV and 130kV), and hence beam fluxes, it was possible to examine the validity of  $\Gamma$  as a physical parameter. From [1] the time evolution of the pressure,  $P$ , in the duct is given by:

$$\frac{dP}{dt} = \frac{Q_0}{V} + \frac{F_I \phi_B \Gamma kT}{V} + \frac{F_R \phi_B \Gamma kT}{V} - \frac{CP}{V} \quad (1)$$

where  $Q_0 = P_0 C$  and  $P_0$  is the pressure immediately before the beam is switched on due to gas flow from the ion-sources, neutralisers, and from the tokamak (recycling and gas fuelling).  $F_I$  and  $F_R$  are the fractions of the transmitted beam flux,  $\phi_B$  (particles  $s^{-1}$ ), that are directly intercepted on the walls or re-ionised respectively,  $C$  is the gas conductance out of the duct of volume  $V$ . It may be shown [1] that a steady-state solution exists for  $\Gamma < \Gamma_{CRIT}$  where

$$\Gamma_{CRIT} = \frac{C}{\phi_B \sigma_{01} L} \quad (2)$$

and  $\sigma_{01}$  is the cross-section for beam re-ionisation in beam-gas collisions. The steady state solution of equation (1) can be written:

$$P = \frac{Q}{C - \sigma_{01} L \phi_B \Gamma} \quad (3)$$

where  $Q$  is the sum of  $Q_0$  and the flow equivalent due to gas re-emission (characterised by coefficient  $\Gamma$ ) from direct interception, where the beam re-ionisation fraction  $F_R = N \sigma_{01} L$  with  $N = P/kT$ , i.e. it is assumed that the re-ionisation takes place over a characteristic length  $L$ . The time-dependent solution to equation (1) is of the form of an exponential rise towards the steady-state pressure, which is the general form of the measured duct pressure during a beam pulse. The time constant of the transient phase is typically  $< 0.5s$ , which is followed by a quasi-steady phase for the remainder of the pulse duration (up to 10s), during which the duct pressure usually continues to rise slowly (*FIG. 2*). In terms of the gas balance model, this is equivalent to a slowly increasing value of  $\Gamma$ . Because the duct protection is essentially uncooled during the pulse, the temperature continues to rise approximately linearly with time, and can reach values  $> 500^\circ C$  in long pulses where the re-ionisation power is highly focused. It is reasonable that  $\Gamma$  should rise with temperature, especially in regions that are heated to high temperatures following long term exposure to particle flux at lower temperatures; this is typically the case for localised re-ionisation hotspots whose position continually varies according to precise plasma parameters and conditions. When strictly identical plasma and beam pulses are run (even in a well-conditioned duct) there is an indication that the implied temperature dependence and the pressure reduce gradually from pulse to pulse (*FIG. 2*). It may be shown that equation (3) may be applied to the quasi-steady phase, providing that the pressure time-derivative is small compared with the initial transient, to obtain  $\Gamma(t)$  and hence the dependence on surface temperature  $\Gamma(T)$ , since  $T(t)$  is available either from thermocouple measurements, or from ion trajectory calculations of the re-ionisation power density distribution and a thermal model of the duct plate. Results are plotted separately for the low and high current beamlines (*FIGS. 3 and 4*). The results are systematically different, and imply that the gas re-emission is *not* proportional to incident beam flux for the two cases at the same surface temperature, i.e.  $\Gamma$  is not a good physical parameter to use for extrapolation in beam flux and  $T$ . Since the EP2 NB enhancement is achieved through a large increase in beam flux, from improved neutralisation of molecular ions and improved transmission [3], an alternative description was sought. It was therefore postulated that a term,  $Q_T(T(t))$ , be included that describes the effective rate of *thermal* re-emission of gas from the hot walls of the duct liner (at temperature  $T$ ) in excess of that due to  $\Gamma$ . For slowly varying  $Q_T(t)$  Equation (3) now takes the approximate form:

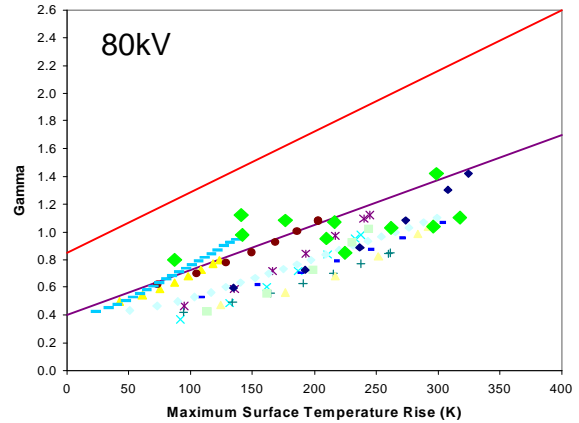
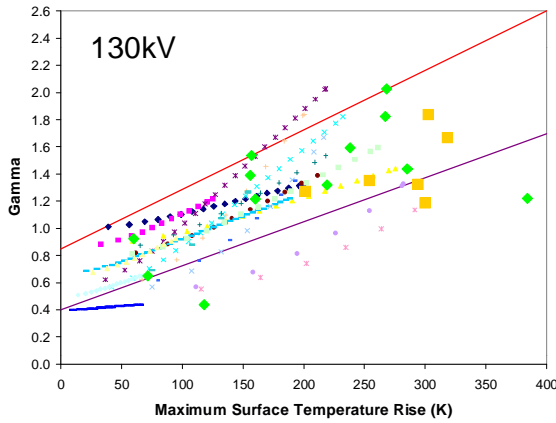


FIG. 3  $\Gamma$  vs.  $T$ , for low flux 130kV beams. Large diamonds and squares: thermocouple data: small symbols and trajectories:  $T$  from Monte Carlo code. Straight lines: range used in first assessment of actively cooled duct design.

FIG. 4  $\Gamma$  vs.  $T$ , for high flux 80kV beams. Large diamonds: thermocouple data: small symbols and trajectories:  $T$  from Monte Carlo code. Straight lines: as in FIG. 3 highlighting systematic reduction in  $\Gamma$  cf. low flux beams at the same  $T$ .

$$P^*(t) = \frac{Q + Q_T(t)}{C - \sigma_{01} L \phi_B \Gamma} \quad (4)$$

so that  $Q_T(T(t))$  could be derived from the pressure rise in the duct. A fixed value  $\Gamma=0.5$  was chosen because (a) this corresponds to unity recycling of the incident beam flux (b) the postulated *additional* thermal re-emission flux is expected to vanish at zero temperature rise, consistent with the value of  $\Gamma \approx 0.5$  at zero temperature rise  $T$  (FIGS. 3 and 4). The resulting  $Q_T(T)$ , derived from thermocouple measurements of the maximum hotspot temperature due to re-ionisation is shown in FIG. 5 and was used [2] to compute the self-consistent combination of surface temperature and duct pressure for a given heat-transfer coefficient and worst-case re-ionisation power density distributions. The heat-transfer performance of the actively cooled duct could therefore be derived, as necessary to maintain an acceptable safe operating margin against fatigue and burnout. However, although the low and high beam flux data were brought together there was still considerable scatter in the data.

### 3. Improved Thermal Re-emission Model

Physically, it is reasonable to assume that  $Q_T$  must depend on the area of the hotspot as well as its temperature. It is worth pointing out that introducing the area into the duct gas release model is a novel feature; the area was a redundant parameter when the gas release was expressed, as in the past, simply as a multiplier of the total re-ionised particle flux, whatever its distribution. Given that the underlying temperature dependence of  $Q_T$  is linear in (FIG. 5), it is postulated that:

$$Q_T \propto \int T dA \quad (6)$$

From the 3D trajectory calculations, the area bounded by the contour representing a re-ionised power density equal to 20% of the computed peak value,  $A_{20}$ , was taken because noise on thermocouple measurements in the low power regions can cause the complete integral to diverge. Multiplying by the average surface temperature rise of the duct,  $T_{ave}$ , allows the re-emission equivalent flow,  $Q_T$ , to be plotted as function of the product  $A_{20}T_{ave}$  as shown in FIG. 6. The linear nature of the relationship (at least for  $A_{20}T_{ave} < 20$ ) is obvious, and the fact

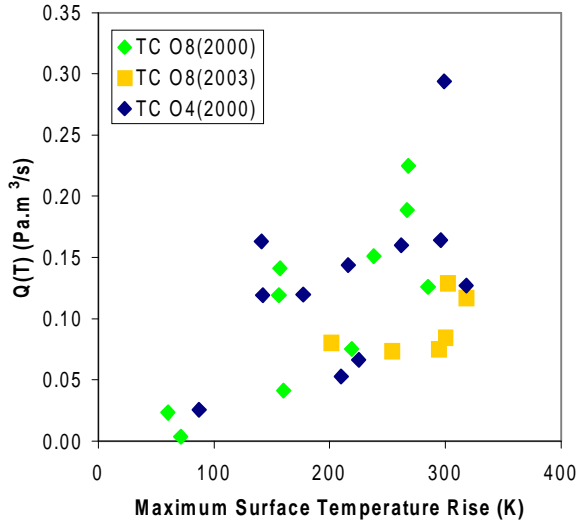


FIG 5  $Q_T$  vs maximum surface temperature rise from thermocouple measurements for 130kV beams (Octant 8) and 80kV beams (Octant 4),

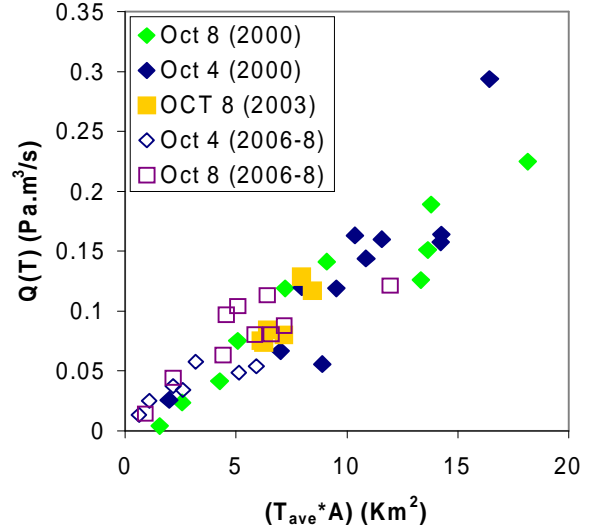


FIG. 6  $Q_T$  vs. product of area within computed 20% duct power density and average temperature from thermocouple measurements for 130kV beams (Octant 8) and 80kV beams (Octant 4)

that the data presents pulses spanning eight years of operation with different beam energy and current combinations emphasises the universal nature of the curve. Only data from pulses with a well-conditioned duct are included, for which the magnetic scenario is well documented, and the re-ionisation hotspot is known to be close to a thermocouple (from detailed 3D trajectory calculations). It is also important to exclude pulses for which there are significant changes in torus conditions during the beam pulse (e.g. fuelling, effect of large MHD events including ELMs, recycling), otherwise, the constant value of  $Q_0$  derived from the pre-beam duct pressure is invalidated and the duct pressure can respond strongly.

#### 4. Assessment of Possible Physical Gas Re-emission Processes

In this section, different simplified models for hydrogenic retention and release mechanisms are considered and tested against the basic features of the experimental observations. These models are not worked out or validated in detail but may help to guide relevant future R&D and modelling. The first model considers only diffusion/recombination of atomic hydrogen which can bind to trap sites. The second model considers molecular hydrogen held in voids due to material damage caused by beam irradiation.

##### 4.1. Diffusion and Recombination

Hydrogenic transport through *undamaged* metals occurs as a result of mobile *atoms* which diffuse through the metallic crystal lattice. Mobile atoms are those which are not bound at trap sites. The binding energy of atoms at the trap sites is of order fraction of an electron-volt and atoms may be promoted to the untrapped or mobile population by raising the temperature or by collision with incoming energetic particles. Depending on conditions (e.g. temperature) undamaged material contains both trapped and mobile hydrogenic atom populations. The mobile population diffuses to the surface according to its concentration gradient. The atoms cannot leave the surface until they have recombined into molecules. Depending on the conditions (temperature and gas release rate), the transport is either *diffusion* or *recombination* limited according to the temperature variation of the diffusion coefficient and the surface

recombination rate-coefficient. The transport in Cu at temperatures relevant to the JET duct liner is *diffusion* limited [4]. Promotion of trapped hydrogen into the mobile population is in principle a possible explanation for the observed behaviour, providing that the characteristic diffusion time is comparable with or longer than the beam pulse length. As the temperature rises, the detrapped hydrogen would then raise the concentration gradient of the mobile population, and the resulting diffusive flow to the surface and release rate would increase with temperature. The values of diffusion coefficient,  $D$ , for deuterium in Cu at room temperature and 200°C are, respectively,  $1.5 \times 10^{-13} \text{ m}^2\text{s}^{-1}$  and  $6 \times 10^{-11} \text{ m}^2\text{s}^{-1}$  [5]. For a typical penetration depth  $\lambda \approx 0.8 \mu\text{m}$  for 100keV D, the characteristic diffusive transport time  $\tau = \lambda^2 / D \approx 10\text{ms}$  at 200°C. This is much less than the beam pulse length, and the diffusive release mechanism of hydrogen displaced from trap sites cannot therefore explain the observed behaviour. In any case, the number of trap sites within the penetration depth over the beam footprint is too low by a factor of order 10 compared with the total gas release in a pulse (see section 4.2. below). The quantity of gas capable of being adsorbed as monolayers and therefore releasable at the surface is also too low, by a factor  $\approx 100$ .

#### 4.2. Release from Gas Bubbles in Material Damaged by Beam Irradiation

It is well established from high-fluence beam-target neutron measurements that the deuterium within the implantation layer reaches large saturation densities  $n_{\text{sat}}$  of order 10% of the Cu atom density, i.e.  $\approx 8 \times 10^{27} \text{ m}^{-3}$  [4,5]. It is also observed that the value of  $n_{\text{sat}}$  varies approximately as  $1/T$  [5]. It may be noted that the density of trap sites (at which hydrogenic atoms may bind) in *undamaged* Cu material is at least an order of magnitude lower than the value of  $n_{\text{sat}}$  inferred from the neutron measurements in high-fluence experiments e.g. [6,7]. Release of occluded gas in the voids caused by beam irradiation at high fluence is the most likely candidate process to be considered. In this case, the hydrogenic species are trapped in the gas phase i.e. as molecules at pressures  $\approx 10^7 \text{ Pa}$ . The transport and release mechanisms do not therefore include atomic diffusion or surface recombination, rather a pressure driven flow under conditions where the mean free path is much less than the characteristic void dimension of 0.1-1 $\mu\text{m}$ . The transport mechanism in this case might be compared with percolation of gas through porous material. Let us assume that the gas released from the bubbles as the temperature is raised is instantaneously emitted, i.e. we neglect finite transport time to reach the surface. We would then have  $Q \propto -dn_{\text{sat}}/dt = -d/dt (\alpha/T)$  where  $\alpha$  is a coefficient of proportionality. Therefore,  $dn_{\text{sat}}/dt = \alpha / T^2 \times dT/dt$ . Since  $dT/dt \approx \text{constant}$  during a pulse, the above implies  $Q \propto 1/T^2$ , in contradiction to the basic experimental result  $Q_T \propto \Delta T$ . We therefore conclude that *instantaneous* release of gas displaced from voids in the damaged material does not occur. It may then be postulated that raising the temperature causes a proportional transient increase in the pressure within the voids, beyond the apparent pressure limit inferred from the  $1/T$  dependence of  $n_{\text{sat}}$  in the steady-state. This would lead to a corresponding increase in the pressure difference across the porous damage layer connecting with the surface. The percolating flow to the surface would increase directly with temperature, and could further indirectly increase via the effect on the voids in the porous layer from changes in thermal and pressure driven stresses. This provides a plausible explanation for the observed behaviour in the duct under the further assumptions: (i) there are large areas of the duct that see low power (and hence particle flux density), arising from the diffuse component of the beam re-ionisation, and can accumulate high  $n_{\text{sat}}$  values characteristic of the low temperature; (ii) hot-spots move onto the previously cooler zones and cause gas to be released. Time dependent pressure measurements for neutral beams impinging on the JET Test Bed beam dumps [4] showed initial net pumping at beam turn-on, followed by net gas release as the beam dump target elements approached their steady-state temperature. This

behaviour also fits the postulated release mechanism. There is an important difference compared to the NBD case however, as the beam power footprint on the Test Bed dumps is the same from shot to shot, and hence each dump region achieves its own value of  $n_{\text{sat}}$ , characteristic only of the repeatable temperature at the end of the pulse. The same is true for the *direct interception* zones of the NBD which do not move significantly. The temperature dependence of  $n_{\text{sat}}$  is also demonstrated by the neutron measurements. A further test of the plausibility of the postulated gas source concerns the amount of gas released from the duct in a long JET beam pulse. The material volume determined by the area of the footprint and the implantation depth must be capable of supplying the observed quantity of gas emitted. For typical value  $A_{20} \approx 0.11 \text{m}^2$ , penetration depth  $\lambda \approx 0.8 \mu\text{m}$ , and  $n_{\text{sat}} = 8 \times 10^{27} \text{m}^{-3}$  (10% Cu atom number density, typical value from neutron measurements with high-fluence targets) we have total available number of atoms  $N_{\text{sat}} = n_{\text{sat}} \lambda A_{20} = 7 \times 10^{20}$  atoms. The time taken to release this amount of gas at  $0.2 \text{Pam}^3 \text{s}^{-1}$  (FIG. 6), as  $\text{D}_2$  molecules, is 6.6s. This is roughly consistent with the observation of no saturation or reduction in gas release (from duct pressure evolution) during long pulses up to 10s. It does, however, raise the possibility of duct pressure starting to recover in beam pulses of  $\gg 10$ s duration or in repeated identical pulses (FIG. 2).

## 5. Gas Re-emission Model Considerations for ITER Electrostatic Ion Dump (ERID)

The copper ERID panels are designed to operate with a maximum surface temperature of  $\sim 300^\circ\text{C}$  and the equivalent value of  $A_{20} T_{\text{ave}}$  for the ERID can be computed from the power density curves given in the ITER DDD [8], the spread of the deflected beam footprint on the ERID panel and the vertical beam height. Scaling from the linear fit to the data of FIG. 6 to the ERID values gives a re-emission equivalent flow estimate of  $1.7 \text{Pam}^3 \text{s}^{-1}$ . According to the analysis in [9] this is still not sufficient to drive the ERID into sustained plasma formation where the beams will not be deflected. For the ITER Diagnostic Neutral Beam (DNB), scaling the panel temperature with beam power implies a density of  $4 \times 10^{18} \text{m}^{-3}$  which could place the DNB into the region of sustained plasma. In applying this gas release description to the ITER beamline ERID, the situation is probably much closer to that of the JET NB Test Bed beam dump, where the footprint shapes are unchanging. Assuming irradiated material with occluded gas that has been initially loaded during low-power operation e.g. during re-start commissioning, the gas release should therefore peak after only a short period of high-power beam operation (i.e. conditioning), to be followed by a period of declining pressure. The relevant parameters defining the characteristic time  $\tau$  for desorbing the occluded gas for the HNB and DNB ERID panels are 40s and 23s respectively, from the arguments of section 4.2.

## 6. Gas Re-emission Model Applied to ITER HNB Duct

The total re-ionised beam fraction in ITER is predicted to be about 4% [8], of which 0.48MW (or 0.48A particle flux) is incident on the duct liner [10]. Trajectory calculations performed at Culham with the BTR code for standard ITER scenarios indicate a value  $A_{20}$  of about  $0.27 \text{m}^2$  for the re-ionised power distribution. The average power density  $P_{\text{ave}}$  within the 20% contour is however much less than in the JET case. The peak power density in the worst case is about  $0.14 \text{MWm}^{-2}$ , and the value of  $P_{\text{ave}} A_{20}$  is about 20kW. This is far less than the total re-ionised power and shows that in the ITER case the majority of the power is outside the 20% contour i.e. is unfocused. This value of  $P_{\text{ave}} A_{20}$  may be translated into a corresponding value  $T_{\text{ave}} A_{20} = 1.6 \text{m}^2 \text{K}$  assuming an appropriate heat transfer coefficient and typical distance of 1cm to the cooling channel in the reference duct liner design [10] of cast copper plates with stainless steel cooling tubes. Using the slope of the trend (FIG. 6) this corresponds to a gas source  $Q_{\text{T}}$  of  $0.024 \text{Pam}^3 \text{s}^{-1}$ , equivalent to dumping an *additional* 2A of beam ions which

return as molecules. Compared with the  $\approx 0.5A$  actual re-ionised flux this implies an effective value  $\Gamma \approx 5$ . Due to the low re-ionisation cross-section at 1MeV and the low beam current,  $\Gamma_{\text{CRIT}}$  is of the order several tens so the duct should remain far away from the blocking condition. In any case, providing the magnetic scenario remains constant for long portions of the discharge,  $Q_T$  should reduce according to the arguments of section 4.2. The capacity of the particle reservoir scales with implantation range (assuming constant void fraction). For an implantation depth of  $\lambda \approx 6\mu\text{m}$  with 1MeV D beams, the time to deplete the reservoir will be higher for a given release rate.  $Q_T$  might be expected to increase with reservoir capacity, but the greater percolation distance to the surface means  $Q_T$  is likely to scale more weakly than linear with  $\lambda$  at a given temperature.

## 6. Conclusions

A new description of thermal gas release from heated surfaces of beamline components exposed to beam fluxes has been developed and benchmarked using JET NBD measurements. The new model takes into account the dimensions and shape of the power distribution, unlike earlier models which relied on a global re-emission coefficient. These new features make the model much better suited to large extrapolations in scale and in beam characteristics, especially particle flux. When applied to the ITER ERID and NBD situations, no new problems are identified. The model can be interpreted in terms of a physical model of gas accumulated in material voids resulting from beam-irradiation damage, and this suggests the gas source may condition away on time-scales shorter than an ITER pulse.

## Acknowledgment

This work was funded jointly by the United Kingdom Engineering and Physical Sciences Research Council and by the European Communities under the contract of Association between EURATOM and UKAEA. The views and opinions expressed herein do not necessarily reflect those of the European Commission.

## References

- [1] Bickley A. et al., Proc 13th Symp. on Fusion Engineering (1989) Knoxville, USA, IEEE, (1990) 1438
- [2] Wilson D. J. et al., (Proc. 13th Symp. on Fusion Technology, Warsaw, Poland, pub. Elsevier 2006) Fusion Engineering and Design, **82** (2007) 845
- [3] Ciric C. et al., (Proc. 13th Symp. on Fusion Technology, Warsaw, Poland, pub. Elsevier 2006) Fusion Engineering and Design, **82** (2007) 610
- [4] Falter H.-D., Gas Absorption, Re-emission and Permeation in Beam Stopping Panels, JET-DN-C(88)57, JET JOINT UNDERTAKING, Abingdon (1988)
- [5] Jones T. T. C. et al., Nucl. Fusion, **46**, (2006) S352
- [6] Kim J., Nucl. Technology, **44**, (1977) 315
- [7] Kim J., Nucl. Instrum. Methods, **145**, (1979) 9
- [8] ITER, Design Description Document 5.3, N 53 DDD 29 01-07-03 R0.1
- [9] Surrey E., et al., Proc. Negative Ion Beams and Sources, Aix-en-Provence (2008), pub. AIP, in press.
- [10] Panasenkov A. A., Analysis of the Heat Loads on the NB Ports Components and Optimization of the Liner Configuration, Final Report, ITER Task Agreement G 15 TD 62 FR, RUSSIAN RESEARCH CENTRE KURCHATOV INSTITUTE, Moscow (2006)